Title

Genome-wide analysis on Chlamydomonas reinhardtii reveals the impact of hydrogen peroxide on protein stress responses and overlap with other stress transcriptomes

Journal

The Plant Journal, 84(5)

ISSN

0960-7412

Authors

Blaby, Ian K
Blaby-Haas, Crysten E
Pérez-Pérez, María Esther
et al.

Publication Date

2015-12-01

DOI

10.1111/tpj.13053

Peer reviewed

the plant journal

SEB Society for Experimental Biology

The Plant Journal (2015) **84,** 974–988 doi: 10.1111/tpj.13053

Genome-wide analysis on *Chlamydomonas reinhardtii* reveals the impact of hydrogen peroxide on protein stress responses and overlap with other stress transcriptomes

Ian K. Blaby[1,†,‡,*], Crysten E. Blaby-Haas[1,†,‡], María Esther Pérez-Pérez[2,§], Stefan Schmollinger[1], Sorel Fitz-Gibbon[3], Stéphane D. Lemaire[2] and Sabeeha S. Merchant[1,3]

[1]*Department of Chemistry and Biochemistry, University of California, Los Angeles, CA 90095, USA,*

[2]*Sorbonne Universités, UPMC Univ. Paris 06, CNRS, UMR8226, Laboratoire de Biologie Moléculaire et Cellulaire des Eucaryotes, Institut de Biologie Physico-Chimique, 75005 Paris, France, and*

[3]*Institute for Genomics and Proteomics, University of California, Los Angeles, CA 90095, USA*

Received 21 September 2015; accepted 7 October 2015; published online 16 October 2015.

*For correspondence (e-mail iblaby@bnl.gov).

[†]These authors contributed equally.

[‡]Present address: Biology Department, Brookhaven National Laboratory, 50 Bell Avenue, Building 463, Upton, NY 11973, USA.

[§]Present address: Instituto de Bioquímica Vegetal y Fotosíntesis, Consejo Superior de Investigaciones Científicas (CSIC)-Universidad de Sevilla, Seville, Spain.

SUMMARY

Reactive oxygen species (ROS) are produced by and have the potential to be damaging to all aerobic organisms. In photosynthetic organisms, they are an unavoidable byproduct of electron transfer in both the chloroplast and mitochondrion. Here, we employ the reference unicellular green alga *Chlamydomonas reinhardtii* to identify the effect of H_2O_2 on gene expression by monitoring the changes in the transcriptome in a time-course experiment. Comparison of transcriptomes from cells sampled immediately prior to the addition of H_2O_2 and 0.5 and 1 h subsequently revealed 1278 differentially abundant transcripts. Of those transcripts that increase in abundance, many encode proteins involved in ROS detoxification, protein degradation and stress responses, whereas among those that decrease are transcripts encoding proteins involved in photosynthesis and central carbon metabolism. In addition to these transcriptomic adjustments, we observe that addition of H_2O_2 is followed by an accumulation and oxidation of the total intracellular glutathione pool, and a decrease in photosynthetic O_2 output. Additionally, we analyze our transcriptomes in the context of changes in transcript abundance in response to singlet O_2 (O_2^*), and relate our H_2O_2-induced transcripts to a diurnal transcriptome, where we demonstrate enrichments of H_2O_2-induced transcripts early in the light phase, late in the light phase and 2 h prior to light. On this basis several genes that are highlighted in this work may be involved in previously undiscovered stress remediation pathways or acclimation responses.

Keywords: H_2O_2, oxidative stress, stress responses, redox signaling, reactive oxygen species, RNA-seq.

INTRODUCTION

Reactive oxygen species (ROS) are potentially harmful but unavoidable byproducts of aerobic respiration and oxygenic photosynthesis. One of the major sources of ROS in the cell is the reduction of univalent O_2 that generates superoxide (O_2^-) in complexes I and III of the mitochondria. In plants, the plastid is an additional source of ROS, where energy transfer within the reaction center of photosystem II (PSII) generates singlet oxygen (O_2^*), and photoreduction of O_2 to O_2^* commonly occurs at photosystem I (PSI) (reviewed in Apel and Hirt, 2004). Although several independent detoxification systems exist, the transient accumulation of ROS is a vital signal that allows the cell to regulate the metabolic processes that generate these toxins and ensure that appropriate protective measures are taken to avoid irreversible damage to proteins, lipids and nucleic acids. The cell can orchestrate the production of enzymes to reduce ROS concentrations and repair damage; otherwise, if the damage is irrevocable, autophagy or apoptosis may ensue.

The ability of H_2O_2 to elicit specific induction or repression of gene expression is well documented (Stone and Yang, 2006; Foyer and Noctor, 2009; Gough and Cotter,

2011). Many of these changes serve to increase the cell's capacity to detoxify H_2O_2, usually through the activity of catalases (to produce H_2O and O_2) or peroxidases (to produce H_2O). Unlike catalase, peroxidase must be reduced by an external electron donor (such as glutathione for glutathione peroxidases) to reduce H_2O_2. Therefore, a common response to H_2O_2 stress is the biosynthesis of antioxidants such as glutathione and ascorbate. Other responses are not necessarily directed at managing H_2O_2 levels but at mitigating the damage produced by H_2O_2. Conserved transcriptional responses include expression of molecular chaperones and increased capacity for protein degradation (Vandenbroucke *et al.*, 2008). Poisoning appears to originate with the Fenton reaction (Walling, 1975), whereby H_2O_2 oxidizes solvent-exposed Fe^{2+}, damaging Fe–S clusters (Jang and Imlay, 2010) and inactivating mononuclear Fe proteins (Sobota and Imlay, 2011; Anjem and Imlay, 2012). In addition to the injury imposed on these susceptible Fe-dependent proteins, the Fenton reaction produces the hydroxyl radical (˙OH), which cannot be enzymatically detoxified and reacts at virtually diffusion-limited rates with most biomolecules. In many ways, H_2O_2 stress can resemble an unfolded protein response, likely due to the misfolding or inactivation of oxidized proteins.

In this study, we employed the single-celled green alga *Chlamydomonas reinhardtii* as a robust system for understanding the global impact of H_2O_2 stress on the transcriptomic landscape in a photosynthesizing cell. In recent years, *Chlamydomonas* has become a favored organism for the interrogation of transcriptional responses to stress through the use of RNA-sequencing (RNA-seq) (González-Ballester *et al.*, 2010; Blaby *et al.*, 2013; Schmollinger *et al.*, 2014; Wakao *et al.*, 2014). In addition to surveying the response of global gene expression to H_2O_2, we validated several of our observations by physiological and biochemical approaches. The wealth of data from previously published transcriptomes in this organism enabled us to contextualize our results with other stresses, allowing us to identify both overlapping and unique responses.

RESULTS

Genome-wide responses to H_2O_2

To capture both intermediate and persistent transcriptional responses, RNA-seq was performed on RNA isolated immediately before (0′), 0.5 and 1 h after the addition of 1 mM H_2O_2 (Figure 1a). Based on the rapid degradation of H_2O_2 from the culture (Figure 1b), we reasoned that primary transcriptional responses would occur within the first hour. Indeed, within 0.5 h, the supernatant concentration of H_2O_2 from the cultures was reduced to about 60% and reduced to background levels after 4 h (Figure 1b). The addition of 1 mM H_2O_2 had no noticeable effect on cell number or growth rate (Figure 1c).

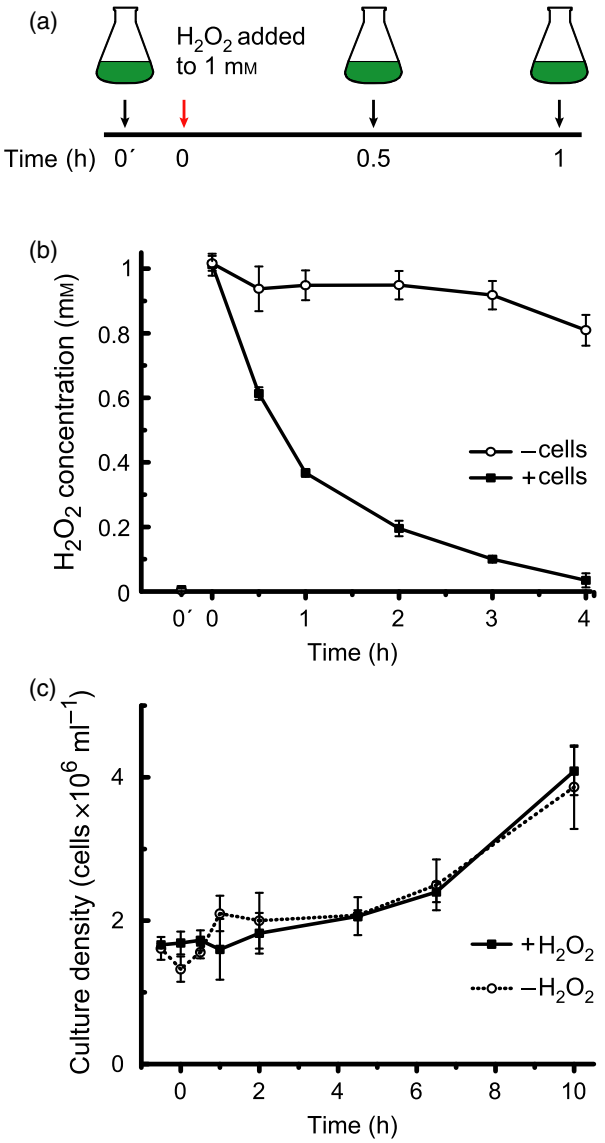

Figure 1. H_2O_2 is rapidly decomposed by *Chlamydomonas*.
(a) For RNA-sequencing analysis, strain CC-4532 was grown to a density of 2×10^6 cells ml^{-1} before collecting an initial sample for RNA preparation (0′). Immediately after this collection, H_2O_2 was added to a final concentration of 1 mM. Subsequent samples were taken at 0.5 and 1 h after H_2O_2 addition.
(b) Concentrations of H_2O_2 were determined by FOX assays. For flasks containing cells, cultures were grown to a density of 2×10^6 cells ml^{-1}. Cell culture supernatant was assayed for H_2O_2 concentration prior to (0′), immediately following (0 h) and at time points subsequent to H_2O_2 addition. Cell-containing cultures are shown in black, cell-free cultures are shown in white.
(c) Cell density measured following H_2O_2 addition. 0′ is defined as the time point immediately prior to H_2O_2 addition, which was added at 0 h. Error bars represent one standard deviation of three measurements.

The sequenced reads were aligned to the v.5 assembly of the *Chlamydomonas* genome (strain CC-503 *cw92 mt*$^+$), and expression estimates were determined for 17 741 (Table S1) loci using the JGI v.5.5 gene models (Merchant

et al., 2007; Blaby *et al.*, 2014). Roughly 7% of predicted transcripts (1278) were differentially abundant [defined as ≥2.0-fold change and ≥10 fragments per kb of exon per million fragments (FPKM)] between any two of the three time points (Table S2). The abundance of 291 transcripts changed between 0′ and 0.5 h (68 down and 223 up), 1251 transcripts between 0′ and 1 h (511 down and 740 up) and 201 transcripts between 0.5 and 1 h (68 down and 133 up).

Based on manual annotation of these transcripts using Pfam domains (Finn *et al.*, 2014), orthology to *Arabidopsis thaliana* and/or *Saccharomyces cerevisiae* (based on reciprocal best Blastp hits) or literature-based functional curation, the highest enriched categories include protein metabolism, nucleotide/nucleic acid metabolism and transcripts that encode proteins related to organelles of the endomembrane system (Figure 2, Table S2). Stress and signaling also factored highly among upregulated functional groups, whereas the tetrapyrrole synthesis and photosynthesis groups decreased in mRNA abundance in all three permutations of comparisons (i.e. 0′–0.5, 0.5–1 and 0′–1). Roughly 13% (73 genes) of the GreenCut, a phylogenetic inventory of chloroplast-related genes (Karpowicz *et al.*, 2011; Heinnickel and Grossman, 2013), was differentially regulated across the time course (between 0′ and 1 h), with 28 decreasing and 45 increasing in transcript abundance (Table S3). Several of those transcripts increasing in abundance encode heat-shock proteins and other stress-related functions, and it is possible that others of currently unknown function have a role in stress remediation (see below and Table S3). Six genes belonging to the CiliaCut (conserved genes amongst ciliated organisms; Merchant *et al.*, 2007) were differentially expressed, all of which decreased in transcript abundance between 0′ and 1 h (although only 165 of the 191 genes

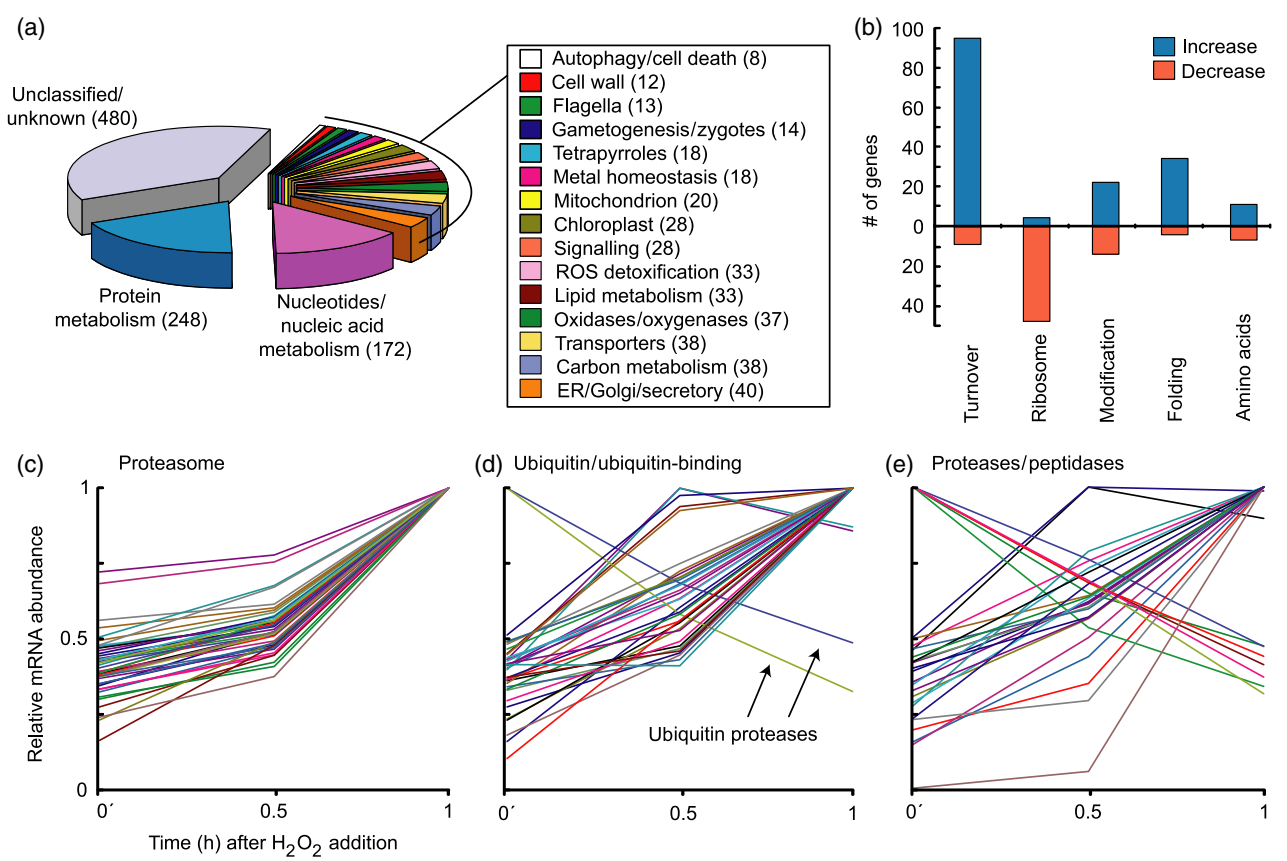

Figure 2. Functional classification of transcripts involved in the H_2O_2 response.
(a) Functional characterization of genes differentially expressed between any two time points. The number of transcripts in each category is shown in parentheses. ROS, reactive oxygen species; ER, endoplasmic reticulum.
(b) The number of genes in each subcategory within the protein metabolism class of panel (a). Increased and decreased mRNA abundances are shown in blue and red, respectively.
(c) Relative transcript abundance of genes encoding components of the proteasome (normalized to the maximum abundance).
(d) Relative transcript abundance of genes encoding ubiquitin and proteins that mediate the ligation (or hydrolysis) of ubiquitin to target proteins. The mRNA abundances are presented normalized to maximum.
(e) Relative transcript abundance of genes encoding putative and known proteases and peptidases (normalized to peak abundance). The fragments per kb of exon per million fragments (FPKM) values can be found in Tables S1 and S2.

in the published CiliaCut, originally defined using the v.3 genome assembly, could be reliably mapped to v.5.5 gene models).

Protein stress

Using both manual annotation and automated MapMan ontologies, the largest proportion of transcripts fell into protein metabolism (Figures 2a,b and S1, Table S2), suggesting a reprioritization of cellular machinery. We found that the transcripts encoding all putative subunits of the 26S proteasome increased in abundance following the addition of H_2O_2 (Figure 2c; 1.8- to 3.3-fold between 0′ and 1 h). This coincided with an increase in 31 transcripts encoding proteins putatively involved in ubiquitination, and a reduction in transcript abundance for two putative ubiquitin-specific proteases (Figure 2d). An impact on protein degradation following the addition of H_2O_2 was not limited to the proteasome–ubiquitin pathway. We also found that the transcript abundance for 22 putative proteases and peptidases increased (while seven decreased) between 0′ and 1 h (Figure 2e). Other indications of protein stress include increased abundance of 38 transcripts encoding either known or putative molecular chaperones and chaperonins (such as *HSP20*, *HSP90*, *HSP70*, *DnaJ* proteins and FKBP-type peptidyl-prolyl *cis–trans* isomerases) across the time course (Table S2). While pathways were induced, presumably to assist in protein folding and initiate protein turnover, 48 transcripts encoding proteins associated with the ribosome, enzymes involved in rRNA processing and ribosome modification/assembly were downregulated, as were transcripts encoding proteins responsible for transcription and several tRNA modifications (Table S2).

Detoxification of ROS

The dual role of H_2O_2 as a harmful by-product of essential oxygenic metabolic reactions and as a signaling molecule necessitates high-fidelity modulation of its presence and concentration within each cellular compartment. Consequently, all aerobic and photosynthetic organisms encode an array of systems charged with ensuring that intracellular H_2O_2 concentrations do not become toxic. Upon exposure to H_2O_2, we observed that several ROS detoxification systems were induced. Although transcripts for some ROS remediation proteins decrease in this experiment, they were already relatively highly abundant at 0′, including transcripts encoding catalases and peroxiredoxins (Figure 3, Table S4). Of the six putative superoxide dismutases (*FSD1* and *MSD1–MSD5*), *FSD1*, *MSD1* and *MSD2* moderately increased in transcript abundance (by about 1.5-fold) with maximal expression estimates at 839, 382 and 116 FPKM, respectively. The transcript level of *MSD3* increased eightfold between 0′ and 1 h, although transcript abundance remained relatively low (peak 24 FPKM). Neither *MSD4* nor

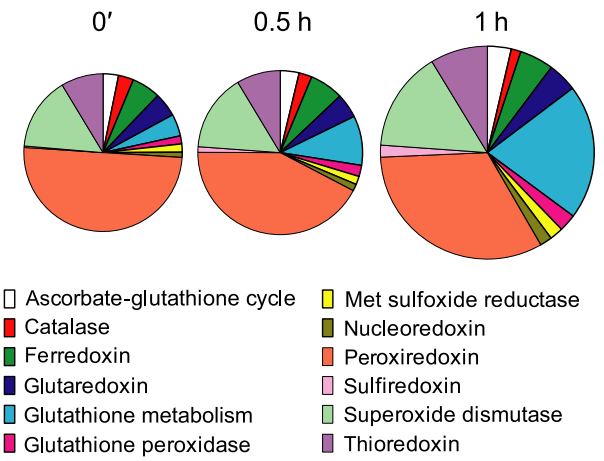

Figure 3. Relative abundance of transcripts putatively involved in detoxification of reactive oxygen species (ROS) subsequent to H_2O_2 addition.
The size of each pie chart is proportional to the total fragments per kb of exon per million fragments (FPKM). Genes and corresponding FPKM values used in this analysis can be found in Table S4.

MSD5, both predicted to localize to the secretory pathway, were expressed (Table S4). The abundance of transcripts encoding three of five glutathione peroxidases did not change. However, *GPX4* and *GPX5* transcripts (encoding non-selenocysteine GPX, and considered to use thioredoxin rather than glutathione as electron donor; Dayer *et al.*, 2008) increased in abundance (peak FPKM values of 20 and 193, respectively). *GPX5* expression was previously shown to be induced by multiple ROS, including H_2O_2, and the corresponding protein was found to reduce H_2O_2 using cytosolic TRXh1, but not GSH, as an electron donor (Leisinger *et al.*, 2001; Fischer *et al.*, 2009). Transcripts encoding proteins putatively contributing to the remediation of ROS damage that were also increased included those encoding nucleoredoxin (*NRX2* and *NRX3*), thioredoxin (*TRXh1*), glutaredoxin (*GRX4*), methionine sulfoxide reductase (*Cre10.g464850*) and, as noted previously (Urzica *et al.*, 2012a), four steps in the Smirnoff–Wheeler pathway for ascorbate biosynthesis (*VTC2*, *MDAR1*, *PNO1* and *DHAR1*).

By contrast, mRNA abundances for 2-*cys* peroxiredoxin-, ascorbate peroxidase- or catalase-encoding genes did not increase following the addition of H_2O_2. Indeed, both *CAT1* and *CAT2* transcripts decreased in transcript abundance over the time course, with *CAT1* transcript being highly abundant at 0′ (197 FPKM) (Table S4). In the case of 2-*cys* peroxiredoxins (for which the abundance of *PRX1* and *PRX2* transcripts was already high at 0′; FPKM > 1300), the capacity for H_2O_2 decomposition may be increased by the induction of two putative sulfiredoxins (encoded by *Cre05.g232800* and *Cre17.g729950*), both of whose transcripts increase in abundance. These proteins can reactivate over-oxidized 2-*cys* peroxiredoxin, a mechanism considered to play an important role in H_2O_2 signal

transduction in mammals (reviewed in Jeong *et al.*, 2012). PRX1 and the sulfiredoxin Cre17.g729950 are predicted to localize to the plastid, while PRX2 and the second putative sulfiredoxin (Cre05.g232800) have no predicted signal peptide (Table S4).

We observed little impact on mRNA abundances of tocopherol (vitamin E), polyamine or carotenoid biosynthesis genes. Each of these pathways has been demonstrated to function in ROS detoxification in other organisms (Havaux *et al.*, 2005; Schneider, 2005; Zhu *et al.*, 2010), although tocopherol acts primarily as a scavenger of O_2^*. Our data suggest that in *Chlamydomonas* these metabolites may not be important for acclimating to short-term H_2O_2 exposure.

Effect of H_2O_2 on glutathione metabolism

As in other organisms, the glutathione redox cycle is expected to play a central role in maintenance of the cellular redox balance. We observed that abundance of *GSH1* mRNA, encoding γ-glutamylcysteine synthetase, the first enzyme in glutathione biosynthesis, increased more than two-fold between 0′ and 1 h (peak FPKM 122). In contrast, the abundance of the mRNA encoding the subsequent enzymatic step, glutathione synthetase (*GSH2*), remained low, and decreased slightly across the time course (Figure 4a, Table S4). To investigate the impact that these transcriptional responses had on glutathione levels, we determined the glutathione pool size in response to H_2O_2 and the proportion present in the oxidized state. We observed both oxidation and accumulation of glutathione after H_2O_2 treatment. The glutathione pool size increased linearly and had more than doubled within 4 h of H_2O_2 addition (Figure 4b). The redox state of glutathione was also altered concomitantly due to the accumulation of oxidized glutathione (GSSG), which resulted in a 50% decrease in the ratio of reduced to oxidized glutathione (GSH/GSSG) within 0.5 h. Within 4 h, this oxidation is partially reversed as the relative proportion of the GSH fraction begins to increase (Figure 4c).

We also observed that the abundance of *GST1* and *GST2* transcripts, encoding two putative glutathione *S*-transferases, was significantly elevated (about 100-fold and 10-fold, respectively, between 0′ and 1 h, each peaking at >700 FPKM) (Figure 4a, Table S4). The expression of both genes was previously found to increase in response to ROS (Fischer *et al.*, 2005). Moreover, consistent with increased sulfur requirements for cysteine production as a precursor for glutathione biosynthesis, we observed slight increases (two-fold at 1 h versus 0′) in expression of a putative cysteine transporter (*AOT4*) and generally for genes encoding enzymes involved in sulfur metabolism.

Photosynthesis

Previous transcriptomic studies on H_2O_2 exposure in land plants and photosynthetic microbes have noted downregulation of genes encoding proteins with roles in photosynthesis (Desikan *et al.*, 2001; Vandenabeele *et al.*, 2003; Zeller *et al.*, 2005). In our dataset, although the change in abundance for most transcripts did not meet our cut-offs, we observed that in general mRNA abundance corresponding to nuclear genome-encoded subunits of photosynthetic complexes was reduced by 30–50% in response to H_2O_2 (Table S5). The abundance of transcripts encoding enzymes of chlorophyll biosynthesis are also generally

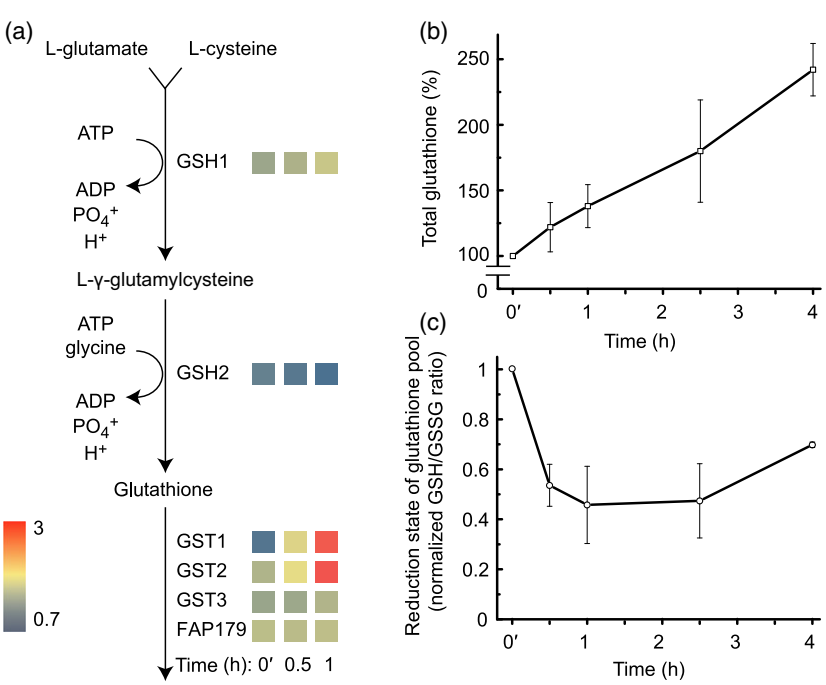

Figure 4. Effect of H_2O_2 on transcripts involved in glutathione metabolism and the glutathione pool.
(a) Transcript abundance of glutathione synthetase 1 (*GSH1*), glutathione synthetase 2 (*GSH2*) and four paralogs of glutathione-*S*-transferase (*GST1–3* and *FAP179*) at 0′ (i.e. immediately prior to the addition of 1 mM H_2O_2), 0.5 and 1 h is shown as a heatmap. The scale bar is in log(FPKM) (FPKM = fragments per kb of exon per million fragments).
(b) Total glutathione, normalized to cellular content at 0′.
(c) Relative proportion of reduced and oxidized glutathione. Error bars represent the standard deviation of at least three independent cultures with three technical replicates for each ($n \geq 9$).

reduced to about 50% at 1 h with respect to their abundances at 0′. In contrast, *CHL1*, which encodes the ortholog of chlorophyllase I in *Arabidopsis*, increased in transcript level three-fold over the same time period. The impact of H_2O_2 on these transcripts correlated with a reduction in photosynthetic efficiency evaluated by measuring the maximum efficiency of PSII and O_2 evolution following the addition of H_2O_2 (Figure 5a,b). Both of these parameters return to pre-H_2O_2 levels after 4 h, at which time the H_2O_2 content of the cell-free supernatant has returned to background levels (Figure 1b), consistent with observations in tobacco (Vandenabeele *et al.*, 2003).

Exceptions to the downward trend include *LHCB7*, encoding a minor antenna protein associated with PSII (Peers and Niyogi, 2008), which increased in abundance by 2.5-fold, peaking at 27 FPKM at 1 h, and *TBA1*, encoding a putative oxidoreductase proposed to regulate translation of *psbA* in response to redox status (Somanchi *et al.*, 2005), which increased in abundance by 3.3-fold, peaking at 61 FPKM. Consistent with their known/predicted role in mitigating photo-oxidative stress, several LHC-like genes rose in transcript abundance during the time course, including *ELIP2* (two-fold induction, peak 13 FPKM) and *ELIP8* (about three-fold induction, peak 162 FPKM) (Table S5).

Respiration

Having observed a reduction in photosynthetic O_2 evolution and in transcript abundance of many genes encoding photosynthetic subunits, we were interested to determine how the mitochondrial electron transport chain (ETC) was affected. Accordingly, we observed a decline in O_2 consumption, with a trough at 0.5 h before recovering to pre-H_2O_2 rates by 2–4 h. However, despite this measurable reduction, the abundance of most transcripts encoding proteins of the mitochondrial ETC does not change (although the transcript level need not necessarily correlate with changes in protein level, or activity) (Table S6). Deviating from this trend are transcripts encoding assembly factors for complex III (BCS1) and complex IV (SCO1, PET191, and CMC1), whose abundances increase between 0′ and 1 h. These increases coincide with the increased abundance of transcripts encoding the alternative enzymes NDA1 (a type II NAD(P)H dehydrogenase) and AOX1 (an alternative oxidase), which increase 2.2-fold (peaking at 31 FPKM) and 4.3-fold (peaking at 96 FPKM), respectively.

Carbon metabolism

The abundances of many transcripts encoding enzymes of central carbon metabolism, including the glyoxylate cycle, glycolysis/gluconeogenesis and the Calvin–Benson (CB) cycle, generally decrease moderately over the time course (Table S7). Coincident with a reduction in O_2 consumption, we observed major reductions in mRNA abundance of a

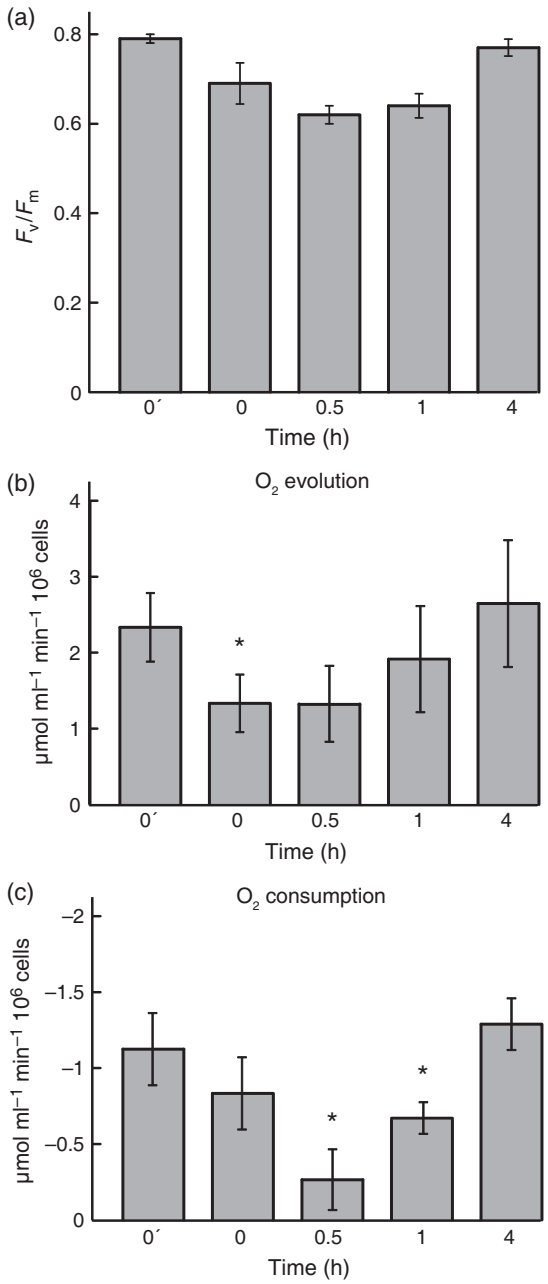

Figure 5. H_2O_2 has a negative impact on photosynthetic and respiratory rates, which recover by 4 h.

(a) F_V/F_M measurements were taken in triplicate (independent cultures) immediately prior to the addition of 1 mM H_2O_2 (0′), immediately after addition (0 h) and at 1, 4 and 8 h subsequently. Error bars indicate ± standard deviation of the three measurements.

(b) Rates of evolution of O_2 in standard growth conditions were determined 0.5 h prior to the addition of 1 mM H_2O_2 (0′), immediately after addition (0 h) and at 1 and 4 h subsequently. Error bars indicate the standard deviation between triplicates (independent cultures), at a starting cell density of 2×10^6 cells ml^{-1}. During measurement, cells were exposed to 75 µmol m^{-2} sec^{-1} light.

(c) The O_2 consumption was determined 0.5 h prior to the addition of 1 mM H_2O_2 (0′), immediately after addition (0 h) and at 1 and 4 h subsequently. Error bars indicate the standard deviation between triplicates (independent cultures), at a starting cell density of 2×10^6 cells ml^{-1}. Significance, indicated by *, was determined by *t*-test ($n = 3$, $P < 0.05$).

few specific metabolism-related genes, specifically those involved in acetate assimilation, including a putative acetate transporter *Cre17.g702900* (Goodenough *et al.*, 2014) and *ACS3* and *MAS1* encoding acetyl-coA synthetase and malate synthase, respectively. Transcripts from these three genes exhibit some of the largest reductions in abundance in the dataset (Table S2) and may reflect a reduced flux of metabolites towards acetyl-CoA, and respiration. In contrast, we observed a slight increase in mRNA abundance of several lipid and starch synthesis genes, likely induced as part of a general stress response (Table S7). Transcript levels of *GPD2*, encoding glycerol-3-phosphate dehydrogenase, and linking carbon assimilation via the CB cycle and gluconeogenesis to lipid synthesis, increased five-fold between 0′ and 0.5 h (FPKM 9 and 66, respectively). Previously, it has been speculated that there may be a link between oxidative stress and the carbon-concentrating mechanism (CCM), based on observations that *CAH1* and *CCP1* were repressed in response to a number of ROS (Ledford *et al.*, 2007). Our data recapitulate these observations, and we observed reduced abundance of *CAH1* transcript (reduced from >500 FPKM at 0′ to 138 at 1 h), and also of *CAH3* transcript (127 and 87 FPKM at 0′ and 1 h, respectively), although this appears not to be a general phenomenon of the CCM as the abundances of other known transcript-encoding components were either stable or increased slightly.

COMPARATIVE TRANSCRIPTOME ANALYSES

Overlap between H_2O_2 and singlet oxygen

We observed a significant overlap in the number of transcripts that increased in abundance following addition of H_2O_2 and rose bengal (RB), which generates O_2^* (Figure 6; Wakao *et al.*, 2014). Roughly 15% of the induced H_2O_2 transcripts between 0′ and 1 h were induced by RB (27% of the RB transcripts in H_2O_2; Table S2). The three most highly represented categories common to both datasets were protein metabolism, proteins related to the endoplasmic reticulum ER/Golgi/secretory pathway and lipid metabolism (Figure 6a). However, only the ER/Golgi/secretory and lipid metabolism groups were significant (*P*-value < 0.001). We noted that the effect on proteasome-subunit transcript abundance and transcripts encoding molecular chaperones (such as heat shock proteins, HSPs) was specific to H_2O_2; the only transcripts encoding HSPs affected by both stresses were *HSP70E*, *HSP70A* and *CPN60C*. The analysis also found that *PTOX1* was increased in both datasets, as was *GPX5* and two nucleoredoxins. Of the top 10 fold-changing transcripts in each pairwise comparison in our H_2O_2 dataset (i.e. 0′ versus 0.5 h, 0′ versus 1 and 1 h versus 0.5 h), only two transcripts were also in the RB dataset: a glutathione *S*-transferase and a protein bearing similarity to the ThiJ family (encoded by *GST1* and *Cre01.g004900*, respectively). H_2O_2, but not RB, affected transcripts involved in tetrapyrrole metabolism (Table S2).

We found a larger (and more significant) overlap between the H_2O_2 response and the RB response in the *sak1* mutant than in the parent ($4A^+$). SAK1 is a putative transcription factor, and disruption of the corresponding gene leads to defective transcriptional responses when the mutant is exposed to O_2^* stress (Wakao *et al.*, 2014). Roughly 25% of the induced H_2O_2 transcripts between 0′ and 1 h were also induced by RB in *sak1*, versus 15% in the parent strain (Figure 6b). To qualify the over-

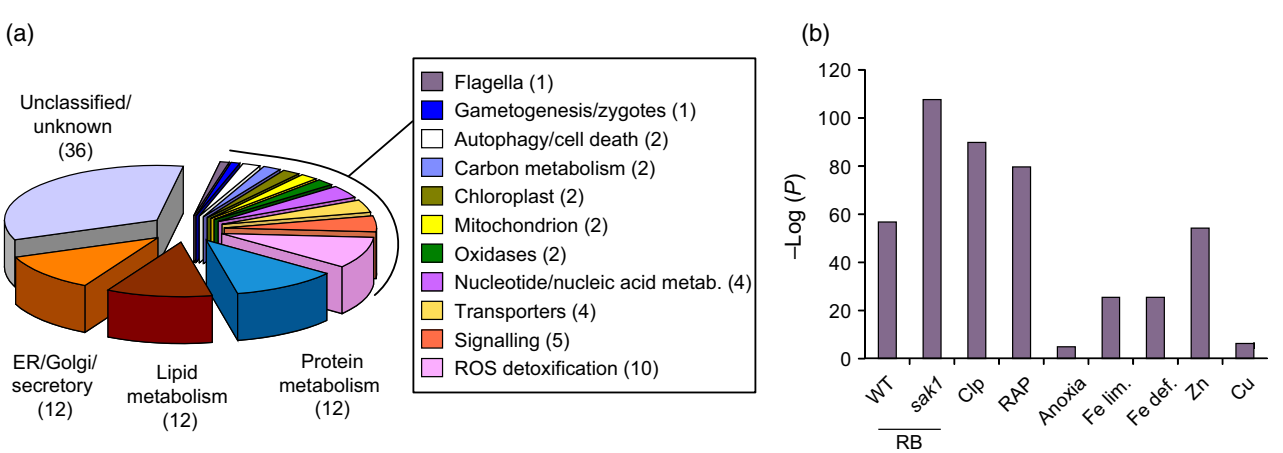

Figure 6. Overlap between the H_2O_2 dataset and published stress transcriptomes.
(a) Functional classification of transcripts whose abundance increased after the addition of H_2O_2 and rose bengal (RB). Numbers in parentheses correspond to the number of transcripts in each category. ROS, reactive oxygen species; ER, endoplasmic reticulum.
(b) *P*-values calculated (using the hypergeometric distribution) for enrichment of H_2O_2 transcripts (induced after 1 h) in several published datasets: wild type (WT) and the *sak1* mutant after RB addition (Wakao *et al.*, 2014), ClpP depletion (Clp), rapamycin addition (RAP; (Ramundo *et al.*, 2014)), growth in dark anoxia (anoxia; Hemschemeier *et al.*, 2013), iron limitation (Fe lim.; Urzica *et al.*, 2012b), iron deficiency (Fe def.; Urzica *et al.*, 2012b), zinc limitation (Zn; Malasarn *et al.*, 2013) and Cu deficiency (Cu; Castruita *et al.*, 2011).

lap between these datasets, we also determined the overlap between the H_2O_2 response and several other transcriptomes that were noted for their enrichment of transcripts related to oxidative stress (ClpP-depletion and poor Fe nutrition; Ramundo *et al.*, 2014; Urzica *et al.*, 2012b) or not (rapamycin-treatment, anoxia, poor Cu nutrition and poor Zn nutrition; Castruita *et al.*, 2011; Hemschemeier *et al.*, 2013; Malasarn *et al.*, 2013) (Figure 6b). We observed both ClpP-depletion and rapamycin treatment (Ramundo *et al.*, 2014) led to a more significant enrichment of H_2O_2-induced transcripts than did addition of RB (based on the *P*-value calculated using the hypergeometric distribution). Conversely, both anoxia and copper depletion had relatively little overlap (Figure 6b). Among these comparisons, the Fe dataset had a moderate overlap, while this analysis revealed a surprisingly large enrichment of H_2O_2-induced transcripts in the Zn-deficient dataset (Figure 6b).

Oxidative stress during the *Chlamydomonas* cell cycle

A recent diurnal transcriptome experiment identified a 'light-stress cluster' of 280 genes that was transiently expressed at the onset of the light phase, but remained near-undetectable across remaining time points (Zones *et al.*, 2015). Of these 280 transcripts, 99 were significantly differentially abundant in response to H_2O_2 in our experiment (56 increased mRNA abundance, 43 decreased between 0′ and 1 h). Next, we determined the time point representing the peak transcript level for each gene in the *Chlamydomonas* genome (using a cutoff of at least 10 FPKM at that point) and analyzed the overlap between the transcripts at each time point and those induced by H_2O_2 addition. Again, we identified an enrichment of H_2O_2-induced transcripts at the first time point in the light. We also observed an enrichment of H_2O_2-induced transcripts with peak values towards the end of the day. We did not observe a significant enrichment during the night except, interestingly, at the 22-h time point (2 h prior to the lights coming on; Figure 7a). For transcripts to which we could assign a general function, the 1-h overlap contained transcripts involved in protein folding and nucleic acid metabolism and binding, whereas towards the end of the day there was an increasing enrichment of transcripts related to protein metabolism, in particular the proteasome. At the 22-h time point there was an enrichment of transcripts related to ROS detoxification/regulation (Figure 7b, Table S8).

For comparative purposes, we repeated this analysis using the RB treatment (parent and *sak1*) and anoxic transcripts in place of our H_2O_2 dataset. As with the comparisons described above, we saw some enrichment of RB-induced transcripts at the 1-h time point and toward the end of the day in both strains, but in contrast to the H_2O_2 dataset the most significant overlap was at the 22-h time point. As expected from the redox status of these cells, we saw no enrichment for anoxia transcripts until the last hour of night.

DISCUSSION

In this study, we have leveraged our transcriptomic analysis to provide a comprehensive overview of the impact that addition of H_2O_2 has on transcript abundance in *Chlamydomonas*. A specific focus on photosynthetic metabolism and ROS detoxification mechanisms provides robust predictions of stress-responsive and remediating genes. In addition, by placing these data in the context of related transcriptomes (Castruita *et al.*, 2011; Hemschemeier *et al.*, 2013; Malasarn *et al.*, 2013; Ramundo *et al.*, 2014; Urzica *et al.*, 2012b; Wakao *et al.*, 2014, Zones *et al.*, 2015) we have been able to identify overlapping responses, potentially highlighting the contribution of ROS stress to independent stimuli. The ability to survey the level of mRNA abundance of all genes provides a powerful tool for assessing the involvement of genes responding to a condition, and thus serves as a means towards hypothesizing roles for genes of previously unknown function.

In the presented work, we identified significant changes in the transcript abundance of 1278 genes, of which 175 have a primary gene symbol and 932 have no known biological role (Table S2). Given this, many of these genes may be of particular interest. They could encode previously undiscovered stress response/ROS detoxification systems, especially considering that the majority increased in transcript abundance; between 0′ and 0.5 h, 223 transcripts increased, as did 740 between 0′ and 1 h, whereas 68 and 511 transcripts decreased between these respective time points (Table S1). One gene that exhibits one of the greatest increases in transcript abundance (at both 0′ versus 0.5 h, and at 0′ versus 1 h) is *Cre03.g152750*, which was induced >80-fold. The predicted protein sequence encodes a BAG domain, associated with apoptosis and programmed cell death (Kang *et al.*, 2006; Kabbage and Dickman, 2008), and a calmodulin-binding domain. That this gene is very lowly expressed (R/FPKM $\leq$ 1) in all but one other published *Chlamydomonas* transcriptome, including RB exposure, suggests it may be responding specifically to H_2O_2 exposure. This notion is supported by its expression profile in a recent diurnal experiment, in which mRNA is detectable at the first light time point, but at no other, and was a member of a light-stress cluster in that work (Zones *et al.*, 2015). *Cre12.g542050* and *Cre04.g226138* are increased in abundance, but do not contain predicted conserved domains and bear no significant similarity to proteins encoded on genomes besides *Chlamydomonas* and the related green alga *Volvox carteri*. The absence of predicted protein domains or clear orthologs in other characterized organisms makes these genes recalcitrant to functional predictions, and future investigation employing approaches such as classical/reverse genetics will be

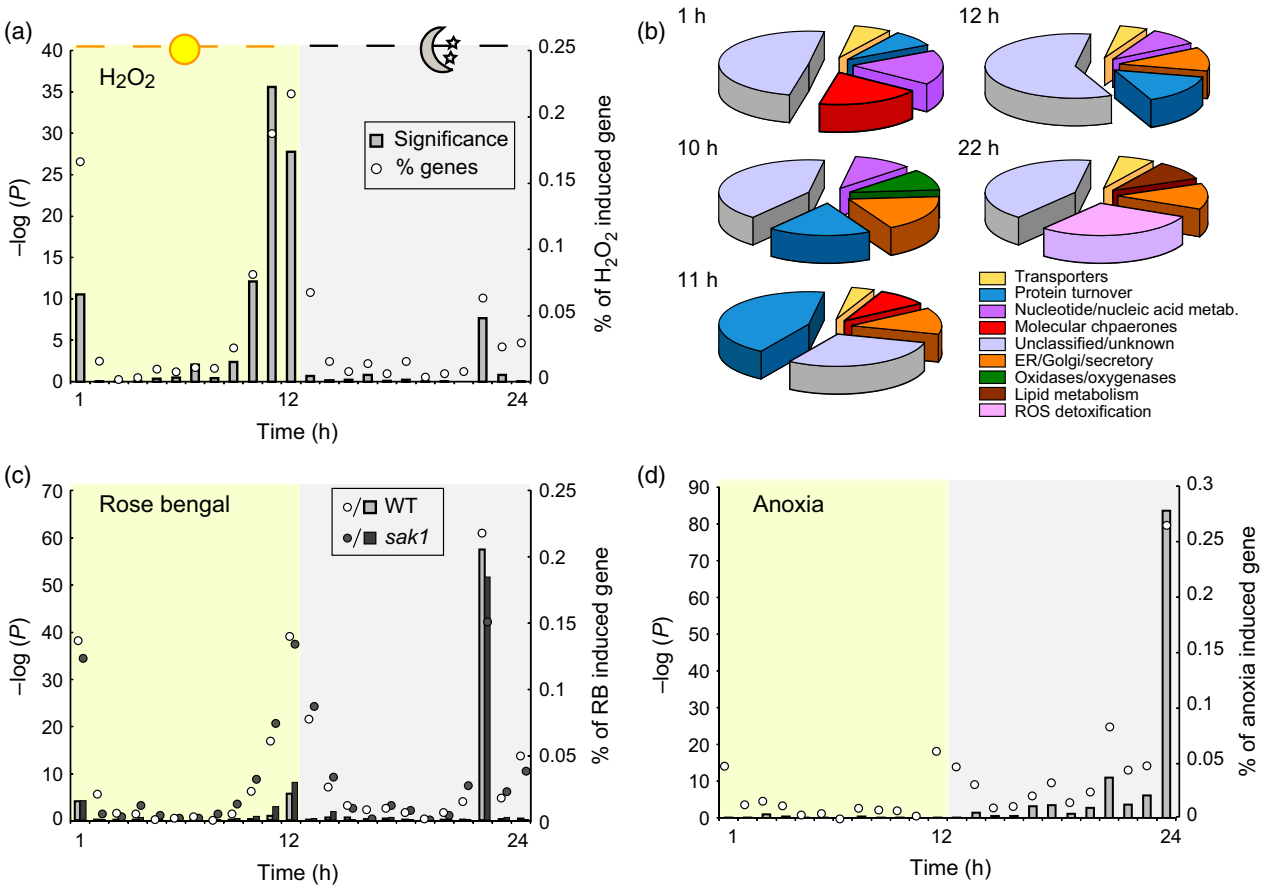

Figure 7. H_2O_2-responsive transcripts during the diurnal cycle.
(a) Analysis of the peak transcript abundance of H_2O_2-induced transcripts during a 12-h diurnal cycle (Zones *et al.*, 2015). *P*-values calculated (using the hypergeometric distribution) for enrichment of H_2O_2-induced transcripts at each time point are presented as a bar graph while the number of H_2O_2-induced transcripts as a percentage of the total number of H_2O_2-induced transcripts are shown as a circle. The 12 h in light is shaded with yellow and highlighted with a sun, while the 12 h in dark is shaded grey and highlighted with a moon.
(b) The top five functional categories containing H_2O_2-induced transcripts at the most significant time points in the cycle. ROS, reactive oxygen species; ER, endoplasmic reticulum.
(c) Same as for panel (a) except that the percentage and associated probability of rose bengal-induced transcripts from the wild type (WT) and the *sak1* mutant is shown.
(d) Same as panel (a) except that the percentage and associated probability of anoxia-induced transcripts is shown.

required to confirm their involvement in ROS detoxification. This analysis also uncovered a previously unrecognized putative ferritin-encoding gene in the *Chlamydomonas* genome. *Cre01.g033300* encodes a protein with high similarity to bacterial DPS (a DNA-binding protein from starved cells), which are ferritin-like proteins responsible for sequestering Fe ions as a means to protect DNA from oxidative damage (Almirón *et al.*, 1992; Pulliainen *et al.*, 2005). Interestingly, in response to H_2O_2 *Cre01.g033300* transcript was increased roughly 10-fold, but the expression estimates remained low (peak 10 FPKM; Table S2), whereas after RB treatment, this transcript increased roughly 80-fold (peak 223 FPKM; Wakao *et al.*, 2014). Also, *Cre01.g033300* is clearly regulated by SAK1 (Wakao *et al.*, 2014), suggesting that Fe-catalyzed DNA damage may be a larger threat from singlet oxygen stress than H_2O_2. Seventy-five genes (45 of unknown function) belonging to the GreenCut inventory, whose phylogenetic profile suggests they are of importance to green photosynthetic organisms, increased in mRNA level in this study. This implicates these genes in having some role in management of ROS stress; indeed, included within this group are several genes previously identified in a light-stress cluster (Zones *et al.*, 2015), as well as numerous characterized stress response enzymes (the largest increase in transcript level is *HSP22A*, whose mRNA abundance increases 176-fold to 58 FPKM at 1 h from 0.3 at 0′). Furthermore, the Arabidopsis ortholog of one GreenCut member, LHCB7, a PSII antenna protein, has been shown to be expressed under conditions of oxidative stress (Alboresi *et al.*, 2011) (mRNA level increase of 2.5-fold in our data across the time course).

In terms of redox detoxification, the transcripts for many quintessential H_2O_2-reducing enzymes did not respond to H_2O_2 treatment, such as ascorbate peroxidase and catalase. Both *CAT1* and *CAT2* transcript abundance were actually reduced over our time course. This is in contrast with other unicellular organisms, such as *S. cerevisiae* or *Synechocystis PCC 6803*, but similar to land plants and mammals (Vandenbroucke *et al.*, 2008). The accumulation and oxidation of glutathione in response to H_2O_2 is commonly observed in most organisms (Vandenbroucke *et al.*, 2008; Noctor *et al.*, 2012). The first step in glutathione synthesis, catalyzed by γ-glutamylcysteine synthetase, is the rate-limiting step (Masip *et al.*, 2006; Noctor *et al.*, 2012; Lu, 2013). The increased expression of *GSH1* in response to H_2O_2 in *Chlamydomonas* may therefore account for the observed accumulation of glutathione. A similar increased expression of this gene was reported in yeast and mammals under diverse stress conditions (Wu and Moye-Rowley, 1994; Lu, 2013). By contrast, in Arabidopsis H_2O_2 does not induce expression of either *GSH1* or *GSH2* but glutathione accumulation appears to involve the induction of genes encoding enzymes involved in cysteine synthesis in the chloroplast (Queval *et al.*, 2009). Interestingly, several of these genes were also induced in *Chlamydomonas* after H_2O_2 addition. All of these results suggest that the mechanisms of redox signaling and detoxification of *Chlamydomonas* are unique since some regulations are shared with higher eukaryotes while others are related to other unicellular organisms. The specificities of *Chlamydomonas* redox metabolism and its responses to hydrogen peroxide may also be linked to the presence, as in mammals, of selenoproteins including glutathione peroxidases, thioredoxin reductases and methionine sulfoxide reductases. Moreover, the site of H_2O_2 accumulation also affects the transcriptional response, as recently shown in Arabidopsis (Sewelam *et al.*, 2014), and exogenous H_2O_2 may not influence the levels of ROS within some compartments significantly. However, the addition of H_2O_2 was clearly able to elicit a generalized reduction in transcripts corresponding to nucleus-encoded photosynthetic complexes and significant remodeling of transcripts related to the endomembrane system. Alternatively, the abundance of catalase transcripts may not be directly related to catalase activity considering the hypothesized role of these proteins in gating H_2O_2 signaling, and the decrease in catalase activity upon addition of H_2O_2, most probably linked to ROS-dependent post-translational regulation (Shao *et al.*, 2008; Michelet *et al.*, 2013).

We noted that a large proportion of transcripts encoding proteins involved in protein folding and degradation increased coordinately with a decrease of transcripts encoding proteins involved in protein synthesis. These trends suggest that the stress caused by addition of H_2O_2 signals a general reduction in cellular activity during the period of exposure, and suggests the potential for global protein remodeling and/or clearance of oxidized proteins following H_2O_2 stress. One possible conclusion is that these systems are induced to clear oxidized proteins with the simultaneous induction of protein degradation and protein folding while protein synthesis is downregulated. Another possibility is that the induction of proteasome transcripts is a result of feedback, since the proteasome and the ubiquitin-activating/conjugating system have been shown to be inhibited by H_2O_2 (Davies, 2001) and by glutathionylation (Demasi *et al.*, 2014). The observed induction in protease transcripts may be responsible for the degradation of oxidatively damaged proteins in compartments and/or a means to compensate for reduced activity of the proteasome.

Moderate reductions in transcript abundance of CB cycle and carbon metabolism genes are consistent with previous reports that algae experience reductions in CO_2 fixation in response to H_2O_2 exposure (Takeda *et al.*, 1995). Reduced abundances of RNAs encoding subunits of the photochemistry machinery were supported physiologically by demonstrating reduced O_2 output subsequent to H_2O_2 exposure. The general reduction observed in transcript level of the photosynthetic machinery is correlated with reduced photosynthetic efficiency at 1 h. Reduction of transcript abundance of photosynthesis-related genes may serve to preserve redox balance and prevent production of additional ROS from photosynthetic electron transport.

Like most plant genomes, *Chlamydomonas* has many gene duplications with paralogs encoding multiple proteins of the same family (Merchant *et al.*, 2007; Wu *et al.*, 2015). As with many other biological processes, the genes encoding enzymes with roles in ROS detoxification are present in up to five or six copies. Unsurprisingly, transcript levels of known ROS-detoxification systems were generally increased, although this pattern of expression was not uniform across all associated paralogs, with transcript abundance corresponding to one gene copy far exceeding that of other copies. For example, expression estimates for *GST1* and *GST2* exceed 700 FPKM, compared with a *GST3* peak of 70. Similar patterns were observed for many paralogous genes. While mRNA abundance does not necessarily translate to protein abundance, and therefore metabolite flux, it does suggest the possibility that some copies have more prominent roles than others.

The importance of understanding ROS-induced damage responses and protective mechanisms has resulted in gene expression studies on H_2O_2 exposure in numerous organisms (e.g. Chuang *et al.*, 2002; Chen *et al.*, 2003; Girardot *et al.*, 2004; Mostertz *et al.*, 2004), including several photosynthetic organisms (Desikan *et al.*, 2000; Vandenabeele *et al.*, 2003; Kobayashi *et al.*, 2004; Li *et al.*, 2004). In a recent meta-analysis, a number of conserved gene families was found to be induced in response to H_2O_2 across lineages

and kingdoms (Vandenbroucke *et al.*, 2008). Our data are largely in agreement with that study: the most highly conserved induced genes were DNAJ-like HSPs, which also increased in mRNA level in our dataset. Three other protein families were found to be induced in all eukaryotes investigated (*A. thaliana*, *S. cerevisiae*, *Schizosaccharomyces pombe* and *Homo sapiens*), including GTP-binding proteins, protein kinases and ubiquitin-conjugating enzymes. In our dataset, genes encoding each of these functions were differentially expressed. However, in our transcriptomes, mRNA abundances for genes encoding both GTP-binding proteins and several protein kinases decreased over the time course, suggesting that the direction of altered expression is not universal. Vandenbroucke *et al.* also observed a conserved induction of short-chain dehydrogenases/reductases and peroxiredoxins in all unicellular organisms in their study (*Synechocystis*, *S. cerevisiae* and *S. pombe*). Our data in *Chlamydomonas*, which is also unicellular, partially support this observation, where transcripts encoding proteins broadly annotated as dehydrogenases/reductases were induced several fold between 0′ and 1 h.

We also compared our H_2O_2 transcriptomes with other relevant *Chlamydomonas* RNA-seq experiments. A recently published O_2^*-response transcriptome allowed us to make a global comparison of these two oxidative stress conditions. Clearly the addition of H_2O_2 and RB elicit independent responses, but we did find a significant overlap highlighting a conserved cluster of stress-related genes. In particular, both ER stress and lipid stress ranked highly among the overlapping transcripts. Indeed, the *Cre01.g004900* transcript level rose in response to both ROS (>50-fold between 0′ and 1 h, peaking at 380 FPKM and three-fold in response to RB) and bears sequence similarity to yeast *HSP31*, encoding a methylglyoxylase, which is also induced in response to oxidative stress (Dubacq *et al.*, 2006). This induction may serve to reduce build-up of methylglyoxal resulting from lipid peroxidation during both stresses.

Interestingly, the overlap between H_2O_2 and RB treatment of the *SAK1* mutant was greater than RB treatment of the wild type. *SAK1* encodes a key regulator of the RB response, and O_2^* exposure of the *SAK1* mutant appears to generate additional oxidative stress that was not observed in the wild type. One possibility is that mis-regulation of SAK1-target transcripts in the presence of RB either exacerbates or leads to a type of oxidative cellular damage in common with H_2O_2. In particular we noticed a substantial increase in the number of transcripts encoding proteins putatively involved in protein turnover in the set of transcripts shared between *sak1* and H_2O_2 (18 transcripts) versus those shared among *sak1*, wild type and H_2O_2 (seven transcripts), suggesting that protein damage could be the point at which the H_2O_2 and *sak1* signaling intersect.

We also observed a large overlap between H_2O_2-responsive transcripts and both ClpP-depletion and rapamycin addition. ClpP is a stromal protease that is thought to play an essential function in the chloroplast (Nishimura and van Wijk, 2015), while rapamycin inhibits TOR signaling, a pathway that promotes cell growth and inhibits autophagy (Dennis *et al.*, 1999). These two transcriptomes were originally performed in conjunction to identify transcriptional changes in the ClpP-depleted strain that are independent of its autophagy-like phenotype (as rapamycin treatment induces autophagy). In this study, we leveraged these datasets to reveal a potential contribution of oxidative stress to the observed transcriptional changes. Indeed, we identified roughly 197 transcripts that increase in abundance following H_2O_2 exposure and ClpP depletion, while nearly 144 transcripts increase in abundance following H_2O_2 exposure and rapamycin treatment. The increase of 94 transcripts was shared between all three datasets. At this point we can only speculate as to whether the significant overlap we observed reflects the ability of ClpP depletion and rapamycin treatment to elicit an oxidative stress response. For instance an obvious physiological intersect is induction of autophagy by the three conditions.

In the diurnal cycle, we found a significant number of H_2O_2-induced transcripts with peak transcript abundance after the transition from dark to light and as cells age during the day. Enrichment within the light stress cluster at the beginning of the day and towards the end of the day was shared with singlet O_2-induced transcripts, but the presence of H_2O_2-induced transcripts was associated with a lower *P*-value. *Chlamydomonas* cells experience an extended G_1 phase during the day, during which biomass is accumulated. Cell division is arrested until the night. Based on functional classification of the corresponding proteins, the H_2O_2-induced transcripts with maximum abundance at the end of day largely encode proteins involved in protein turnover. Unexpectedly, we also observed a spike in ROS-induced transcripts at 2 h prior to the transition to day, possibly highlighting clock-regulated transcripts, which are maximally abundant in anticipation of the transition to the light period. Although there was a significant enrichment of H_2O_2-induced transcripts with peak abundance at this time point, we found a higher significance associated with RB-induced transcripts, possibly highlighting anticipation of photo-oxidative damage associated with the shock of switching from dark to light. The abundance of the *Chlamydomonas* ortholog of Arabidopsis *CCA1* (*Cre06.g275350*; circadian clock-associated 1), demonstrated to regulate the induction of oxidative stress responses in that organism (Lai *et al.*, 2012), is slightly reduced throughout our time course. In the *Chlamydomonas* diurnal experiment peak abundance occurs immediately prior to the light period, suggesting that *Cre06.g275350* is regulated by circadian rhythms here also, and is not influenced by the presence of ROS.

EXPERIMENTAL PROCEDURES

Strains and culture conditions

Strain CC-4532 (Mets strain 2137 *mt*$^-$) was used throughout this study. Routine growth was performed in 2-amino-2-(hydroxymethyl)-1,3-propanediol (TRIS)-acetate–phosphate (TAP) using Hutner's trace element mix (Hutner *et al.*, 1950). Cultures were grown in Innova incubators (New Brunswick Scientific, http://www.eppendorf.com) at 24°C, agitated at 180 rpm with continuous light (95 μmol m^{-2} sec^{-1}, six cool white fluorescent bulbs at 4100K and three warm white fluorescent bulbs at 3000K per incubator). Unless indicated otherwise, freshly aliquotted H_2O_2 (Fisher, https://www.fishersci.com/) was added to cultures to a final concentration of 1 mM at about 2×10^6 cells ml^{-1}. Culture densities (in cells ml^{-1}) were determined with a hemocytometer.

H_2O_2 RNA-seq read realignment and analysis

Transcriptomic data analyzed in this study were initially acquired as described in Urzica *et al.* (2012a). The sequence reads resulting from this previous study were aligned to v.5.5 of the reference genome (Merchant *et al.*, 2007) (available at ftp://ftp.jgi-psf.org/pub/compgen/phytozome/v9.0/Creinhardtii/) using STAR (Dobin *et al.*, 2013), default parameters plus –alignIntronMax 10000 and expression estimates were determined and normalized in terms of FPKM using cuffdiff (Trapnell *et al.*, 2010) default parameters.

F_V/F_M measurements

F_V/F_M measurements were determined using a FluorCam 800MF (Photon Systems Instruments, http://www.psi.cz/). Cells (3×10^7) were sampled from cultures and concentrated onto a Whatman 25-mm circular filter paper disk using a vacuum. Cell-containing filter disks were dark-adapted for 15 min before performing F_V/F_M measurements using FluorCam6.0 software (Photon Systems Instruments).

H_2O_2 degradation (FOX) assays

The concentration of H_2O_2 in culture flasks was determined by FOX assays, as described by Nourooz-Zadeh (1999). Briefly 0.1-ml culture samples were taken from cultures at a cell density of 2×10^6 cells ml^{-1}, or non-inoculated flasks for cell-free control samples. Samples containing cells were centrifuged (16 100 ***g*** for 3 min) and the supernatant transferred to fresh tubes. Then 0.9 ml of FOX assay reagent A (25 mM 93% sulfuric acid, 2.5 mM ammonium iron sulfate, 1 mM xylenol orange) was added, the mixture was incubated at room temperature 24°C for 10 min, and the absorption determined at 560 nm. H_2O_2 concentrations were determined by reading absorption measurements off a standard curve prepared with known concentrations. Measurements were performed on three separate cultures (biological replicates). Measurements were taken at 0 h (immediately after addition of 1 mM H_2O_2), and at 0.5, 1, 2, 3 and 4 h thereafter.

Oxygen consumption and evolution

Oxygen evolution and consumption rates were measured on a standard Clark-type electrode (Hansatech Oxygraph with a DW-1 chamber, http://hansatech-instruments.com/) and the data analyzed with the Hansatech OxyLab software v.1.15. Experiments were performed using 2 ml of culture at 2×10^6 cells ml^{-1} in the presence of 20 mM acetate and 10 mM $KHCO_3$. Samples were taken 0.5 h prior to addition of H_2O_2 (added to a final concentration of 1 mM), immediately after addition (t0), and at 0.5, 1, 2 and 4 h subsequent to addition of H_2O_2. Measurements were performed on three separate cultures (biological repeats). The respiration rate was measured as oxygen consumption over a period of 4 min in the dark. The rate of photosynthetic O_2 evolution was measured for 4 min in the light (75 μmol m^{-2} sec^{-1}) after a 4-min acclimation period and was calculated as the difference between oxygen evolution in the light and oxygen consumption in the dark.

Glutathione pool measurements

Chlamydomonas cells treated with 1 mM H_2O_2 were collected at 0, 0.5, 1, 3 and 4 h by centrifugation (5000 ***g*** for 5 min), washed once in 50 mM sodium phosphate (pH 7.5) solution, resuspended in 0.2 N HCl and lysed by two cycles of freeze/thaw at −80°C. Crude extracts were cleared by centrifugation at 15 000 ***g*** for 20 min at 4°C. Then 500 μl of sample was neutralized by adding 50 μl of 50 mM NaH_2PO_4 (pH 7.5) and 0.2 N NaOH to a final pH of between 5 and 6. The neutralized sample was used directly for measuring total glutathione (GSH plus GSSG) by the recycling assay initially described by Tietze (1969) and adapted from Queval and Noctor (2007). The method relies on the glutathione reductase (GR)-dependent reduction of 5,5′-dithiobis(2-nitro-benzoic acid) (DTNB; Sigma, D8130, http://www.sigmaaldrich.com/). Oxidized glutathione was measured after treatment of a neutralized sample with 10 mM 4-vinylpyridine (VPD; Sigma V320-4) for 30 min at 25°C. To remove excess VPD, the derivatized sample was centrifuged twice at 15 000 ***g*** for 20 min at 4°C. To measure total glutathione or GSSG, the sample was added to a mix containing 120 mM NaH_2PO_4 (pH 7.5), 300 μM DTNB, 500 μM NADPH, 1 mM EDTA (pH 8), 1 U ml^{-1} GR (Sigma, G3664), and DTNB reduction was measured at 412 nm. Different GSH (Sigma, G4251) concentrations ranging from 0 to 5 μM were used as standards. For each time point, three independent biological replicates were measured with at least three technical replicates for each sample. Data are represented as mean ± SD ($n \geq 9$).

Methods for comparative transcriptome analysis

The same cutoffs as those used for the H_2O_2 analysis (i.e. ≥10 FPKM/RPKM, ≥2.0-fold change) were applied to the expression estimates of previously published datasets (Castruita *et al.*, 2011; Urzica *et al.*, 2012b; Hemschemeier *et al.*, 2013; Malasarn *et al.*, 2013; Ramundo *et al.*, 2014; Wakao *et al.*, 2014). The list of upregulated transcripts from each dataset was then compared with the list of transcripts that increased in abundance before and 1 h after H_2O_2 addition (referred to as H_2O_2-responsive). For the ClpP-depletion–H_2O_2 overlap, our dataset was composed of transcripts that met our cutoffs and increased in strain DCH16 after 43 h of vitamin addition. For the rapamycin analysis, our dataset was composed of transcripts that met our cutoffs and increased in A31 (the wild-type strain in that work) after 8 h of rapamycin addition. The *P*-value for each overlap was calculated using *R*, with the command sum(dhyper((*q*:*m*, *k*, 17 301-*k*, *m*))), where *q* is the number of transcripts in the overlap, *m* is the number of transcripts that increased in abundance following addition of H_2O_2 and *k* is the number of transcripts that increased in abundance in the dataset being compared. Because the datasets we used to perform these comparisons were all aligned to the v.4 assembly of the *Chlamydomonas* genome, we converted loci IDs in the H_2O_2 dataset from v.5 to v.4 (which contains 17 301 loci) using the correspondence table available at http://genome.jgi.doe.gov/pages/dynamicOrganismDownload.jsf?organism=PhytozomeV10. For each transcript in the diurnal cycle, we determined at which time point the maximum FPKM value is reached. Transcripts that did

not reach 10 FPKM at any time point were excluded. We then determined the number of H_2O_2-responsive transcripts in each list of maximum FPKMs and calculated the *P*-value associated with the overlap as above.

ACCESSION NUMBERS

Sequenced reads are available on the National Center for Biotechnology Information (NCBI) Gene Expression Omnibus (GEO) database under accession number GSE34826.

ACKNOWLEDGEMENTS

This work was supported by the Division of Chemical Sciences, Geosciences, and Biosciences, Office of Basic Energy Sciences of the US Department of Energy (DE-FD02-04ER15529) and by the National Institutes of Health (NIH) R24 GM092473 to SM. This work was also supported in part by Agence Nationale de la Recherche Grant CYNTHIOL ANR-12-BSV6-0011 and LABEX DYNAMO ANR-11-LABX-0011 (to SDL). IKB and CB-H were supported by training grants from the National Institutes of Health (T32ES015457 and GM100753 respectively) and by the Office of Biological and Environmental Research of the Department Of Energy. MEP-P was supported by an IEF EU Marie Curie Fellowship (PIEF-GA-2011-298652-REDOXDYNAMICS). We are grateful to M. Dudley Page for help with gene curation.

SUPPORTING INFORMATION

Additional Supporting Information may be found in the online version of this article.

Figure S1. Gene Ontology analysis identifies global changes in differentially expressed genes.

Table S1. Expression estimates for all genes.

Table S2. Genes whose mRNA abundance significantly changes in response to H_2O_2.

Table S3. GreenCut genes whose mRNA abundance significantly changes in response to H_2O_2.

Table S4. Messenger RNA abundances for genes encoding enzymes relating to detoxification of reactive oxygen species.

Table S5. Messenger RNA abundances for genes encoding enzymes relating to photosynthesis.

Table S6. Messenger RNA abundances for genes encoding enzymes involved in respiration.

Table S7. Messenger RNA abundances for genes encoding enzymes relating to carbon metabolism.

Table S8. Overlap of differentially expressed genes between H_2O_2, rose bengal and anoxia experiments with a *Chlamydomonas* diurnal cell cycle transcriptome.

REFERENCES

Alboresi, A., Dall'osto, L., Aprile, A., Carillo, P., Roncaglia, E., Cattivelli, L. and Bassi, R. (2011) Reactive oxygen species and transcript analysis upon excess light treatment in wild-type *Arabidopsis thaliana* vs a photosensitive mutant lacking zeaxanthin and lutein. *BMC Plant Biol.* **11**, 62.

Almirón, M., Link, A.J., Furlong, D. and Kolter, R. (1992) A novel DNA-binding protein with regulatory and protective roles in starved *Escherichia coli*. *Genes Dev.* **6**, 2646–2654.

Anjem, A. and Imlay, J.A. (2012) Mononuclear iron enzymes are primary targets of hydrogen peroxide stress. *J. Biol. Chem.* **287**, 15544–15556.

Apel, K. and Hirt, H. (2004) Reactive oxygen species: metabolism, oxidative stress, and signal transduction. *Annu. Rev. Plant Biol.* **55**, 373–399.

Blaby, I.K., Glaesener, A.G., Mettler, T. *et al.* (2013) Systems-level analysis of nitrogen starvation-induced modifications of carbon metabolism in a *Chlamydomonas reinhardtii* starchless mutant. *Plant Cell*, **25**, 4305–4323.

Blaby, I.K., Blaby-Haas, C.E., Tourasse, N. *et al.* (2014) The *Chlamydomonas* genome project: a decade on. *Trends Plant Sci.* **19**, 672–680.

Castruita, M., Casero, D., Karpowicz, S.J. *et al.* (2011) Systems biology approach in *Chlamydomonas* reveals connections between copper nutrition and multiple metabolic steps. *Plant Cell*, **3**, 1273–1292.

Chen, D., Toone, W.M., Mata, J., Lyne, R., Burns, G., Kivinen, K., Brazma, A., Jones, N. and Bähler, J. (2003) Global transcriptional responses of fission yeast to environmental stress. *Mol. Biol. Cell*, **14**, 214–229.

Chuang, Y.Y., Chen, Y., Gadisetti *et al.* (2002) Gene expression after treatment with hydrogen peroxide, menadione, or t-butyl hydroperoxide in breast cancer cells. *Cancer Res.* **62**, 6246–6254.

Davies, K.J. (2001) Degradation of oxidized proteins by the 20S proteasome. *Biochimie*, **83**, 301–310.

Dayer, R., Fischer, B.B., Eggen, R.I. and Lemaire, S.D. (2008) The peroxiredoxin and glutathione peroxidase families in *Chlamydomonas reinhardtii*. *Genetics*, **179**, 41–57.

Demasi, M., Hand, A., Ohara, E., Oliveira, C.L., Bicev, R.N., Bertoncini, C.A. and Netto, L.E. (2014) 20S proteasome activity is modified via S-glutathionylation based on intracellular redox status of the yeast *Saccharomyces cerevisiae*: implications for the degradation of oxidized proteins. *Arch. Biochem. Biophys.* **557**, 65–71.

Dennis, P.B., Fumagalli, S. and Thomas, G. (1999) Target of rapamycin (TOR): balancing the opposing forces of protein synthesis and degradation. *Curr. Opin. Genet. Dev.* **9**, 49–54.

Desikan, R., Neill, S.J. and Hancock, J.T. (2000) Hydrogen peroxide-induced gene expression in *Arabidopsis thaliana*. *Free Radic. Biol. Med.* **28**, 773–778.

Desikan, R., A-H-Mackerness, S., Hancock, J.T. and Neill, S.J. (2001) Regulation of the *Arabidopsis* transcriptome by oxidative stress. *Plant Physiol.* **127**, 159–172.

Dobin, A., Davis, C.A., Schlesinger, F., Drenkow, J., Zaleski, C., Jha, S., Batut, P., Chaisson, M. and Gingeras, T.R. (2013) STAR: ultrafast universal RNA-seq aligner. *Bioinformatics*, **29**, 15–21.

Dubacq, C., Chevalier, A., Courbeyrette, R., Petat, C., Gidrol, X. and Mann, C. (2006) Role of the iron mobilization and oxidative stress regulons in the genomic response of yeast to hydroxyurea. *Mol. Genet. Genomics*, **275**, 114–124.

Finn, R.D., Bateman, A., Clements, J. *et al.* (2014) Pfam: the protein families database. *Nucleic Acids Res.* **42**, D222–D230.

Fischer, B., Krieger-Liszkay, A. and Eggen, R. (2005) Oxidative stress induced by the photosensitizers neutral red (type I) or rose bengal (type II) in the light causes different molecular responses in *Chlamydomonas reinhardtii*. *Plant Sci.* **168**, 747–759.

Fischer, B.B., Dayer, R., Schwarzenbach, Y., Lemaire, S.D., Behra, R., Liedtke, A. and Eggen, R.I. (2009) Function and regulation of the glutathione peroxidase homologous gene *GPXH/GPX5* in *Chlamydomonas reinhardtii*. *Plant Mol. Biol.* **71**, 569–583.

Foyer, C.H. and Noctor, G. (2009) Redox regulation in photosynthetic organisms: signaling, acclimation, and practical implications. *Antioxid. Redox Signal.* **11**, 861–905.

Girardot, F., Monnier, V. and Tricoire, H. (2004) Genome wide analysis of common and specific stress responses in adult drosophila melanogaster. *BMC Genom.* **5**, 74.

González-Ballester, D., Casero, D., Cokus, S., Pellegrini, M., Merchant, S.S. and Grossman, A.R. (2010) RNA-seq analysis of sulfur-deprived *Chlamydomonas* cells reveals aspects of acclimation critical for cell survival. *Plant Cell*, **22**, 2058–2084.

Goodenough, U., Blaby, I., Casero, D. *et al.* (2014) The path to triacylglyceride obesity in the *sta6* strain of *Chlamydomonas reinhardtii*. *Eukaryot. Cell*, **13**, 591–613.

Gough, D.R. and Cotter, T.G. (2011) Hydrogen peroxide: a Jekyll and Hyde signalling molecule. *Cell Death Dis.* **2**, e213.

Havaux, M., Eymery, F., Porfirova, S., Rey, P. and Dörmann, P. (2005) Vitamin E protects against photoinhibition and photooxidative stress in *Arabidopsis thaliana*. *Plant Cell*, **17**, 3451–3469.

Heinnickel, M.L. and Grossman, A.R. (2013) The GreenCut: re-evaluation of physiological role of previously studied proteins and potential novel protein functions. *Photosynth. Res.* **116**, 427–436.

Hemschemeier, A., Casero, D., Liu, B., Benning, C., Pellegrini, M., Happe, T. and Merchant, S.S. (2013) Copper response regulator1-dependent and -independent responses of the *Chlamydomonas reinhardtii* transcriptome to dark anoxia. *Plant Cell*, **25**, 3186–3211.

Hutner, S.H., Provasoli, L., Schatz, A. and Haskins, C.P. (1950) Some approaches to the study of the role of metals in the metabolism of microorganisms. *Proc. Am. Philos. Soc.* **94**, 152–170.

Jang, S. and Imlay, J.A. (2010) Hydrogen peroxide inactivates the *Escherichia coli* Isc iron–sulphur assembly system, and OxyR induces the Suf system to compensate. *Mol. Microbiol.* **78**, 1448–1467.

Jeong, W., Bae, S.H., Toledano, M.B. and Rhee, S.G. (2012) Role of sulfiredoxin as a regulator of peroxiredoxin function and regulation of its expression. *Free Radic. Biol. Med.* **53**, 447–456.

Kabbage, M. and Dickman, M.B. (2008) The BAG proteins: a ubiquitous family of chaperone regulators. *Cell. Mol. Life Sci.* **65**, 1390–1402.

Kang, C.H., Jung, W.Y., Kang, Y.H. *et al.* (2006) AtBAG6, a novel calmodulin-binding protein, induces programmed cell death in yeast and plants. *Cell Death Differ.* **13**, 84–95.

Karpowicz, S.J., Prochnik, S.E., Grossman, A.R. and Merchant, S.S. (2011) The GreenCut2 resource, a phylogenomically derived inventory of proteins specific to the plant lineage. *J. Biol. Chem.* **286**, 21427–21439.

Kobayashi, M., Ishizuka, T., Katayama, M., Kanehisa, M., Bhattacharyya-Pakrasi, M., Pakrasi, H.B. and Ikeuchi, M. (2004) Response to oxidative stress involves a novel peroxiredoxin gene in the unicellular cyanobacterium *Synechocystis* sp. PCC 6803. *Plant Cell Physiol.* **45**, 290–299.

Lai, A.G., Doherty, C.J., Mueller-Roeber, B., Kay, S.A., Schippers, J.H. and Dijkwel, P.P. (2012) CIRCADIAN CLOCK-ASSOCIATED 1 regulates ROS homeostasis and oxidative stress responses. *Proc. Natl Acad. Sci. USA*, **109**, 17129–17134.

Ledford, H.K., Chin, B.L. and Niyogi, K.K. (2007) Acclimation to singlet oxygen stress in *Chlamydomonas reinhardtii*. *Eukaryot. Cell*, **6**, 919–930.

Leisinger, U., Rüfenacht, K., Fischer, B., Pesaro, M., Spengler, A., Zehnder, A.J. and Eggen, R.I. (2001) The glutathione peroxidase homologous gene from *Chlamydomonas reinhardtii* is transcriptionally up-regulated by singlet oxygen. *Plant Mol. Biol.* **46**, 395–408.

Li, H., Singh, A.K., McIntyre, L.M. and Sherman, L.A. (2004) Differential gene expression in response to hydrogen peroxide and the putative *PerR* regulon of *Synechocystis* sp. strain PCC 6803. *J. Bacteriol.* **186**, 3331–3345.

Lu, S. (2013) Glutathione synthesis. *Biochem. Biophys. Acta*, **1830**, 3143–3153.

Malasarn, D., Kropat, J., Hsieh, S.I., Finazzi, G., Casero, D., Loo, J.A., Pellegrini, M., Wollman, F.-A. and Merchant, S.S. (2013) Zinc deficiency impacts CO_2 assimilation and disrupts copper homeostasis in *Chlamydomonas reinhardtii*. *J. Biol. Chem.* **288**, 10672–10683.

Masip, L., Veeravalli, K. and Georgiou, G. (2006) The many faces of glutathione in bacteria. *Antioxid. Redox Signal.* **8**, 753–762.

Merchant, S.S., Prochnik, S.E., Vallon, O. *et al.* (2007) The *Chlamydomonas* genome reveals the evolution of key animal and plant functions. *Science*, **318**, 245–250.

Michelet, L., Roach, T., Fischer, B.B., Bedhomme, M., Lemaire, S.D. and Krieger-Liszkay, A. (2013) Down-regulation of catalase activity allows transient accumulation of a hydrogen peroxide signal in *Chlamydomonas reinhardtii*. *Plant, Cell Environ.* **36**, 1204–1213.

Mostertz, J., Scharf, C., Hecker, M. and Homuth, G. (2004) Transcriptome and proteome analysis of *Bacillus subtilis* gene expression in response to superoxide and peroxide stress. *Microbiology*, **150**, 497–512.

Nishimura, K. and van Wijk, K.J. (2015) Organization, function and substrates of the essential Clp protease system in plastids. *Biochim. Biophys. Acta*, **1847**, 915–930.

Noctor, G., Mhamdi, A., Chaouch, S., Han, Y., Neukermans, J., Marquez-Garcia, B., Queval, G. and Foyer, C.H. (2012) Glutathione in plants: an integrated overview. *Plant, Cell Environ.* **35**, 454–484.

Nourooz-Zadeh, J. (1999) Ferrous ion oxidation in presence of xylenol orange for detection of lipid hydroperoxides in plasma. *Methods Enzymol.* **300**, 58–62.

Peers, G. and Niyogi, K.K. (2008) Pond scum genomics: the genomes of *Chlamydomonas* and Ostreococcus. *Plant Cell*, **20**, 502–507.

Pulliainen, A.T., Kauko, A., Haataja, S., Papageorgiou, A.C. and Finne, J. (2005) Dps/Dpr ferritin-like protein: insights into the mechanism of iron incorporation and evidence for a central role in cellular iron homeostasis in *Streptococcus suis*. *Mol. Microbiol.* **57**, 1086–1100.

Queval, G. and Noctor, G. (2007) A plate reader method for the measurement of NAD, NADP, glutathione, and ascorbate in tissue extracts: application to redox profiling during *Arabidopsis* rosette development. *Anal. Biochem.* **363**, 58–69.

Queval, G., Thominet, D., Vanacker, H., Miginiac-Maslow, M., Gakière, B. and Noctor, G. (2009) H_2O_2-activated up-regulation of glutathione in *Arabidopsis* involves induction of genes encoding enzymes involved in cysteine synthesis in the chloroplast. *Mol. Plant*, **2**, 344–356.

Ramundo, S., Casero, D., Mühlhaus, T. *et al.* (2014) Conditional depletion of the *Chlamydomonas* chloroplast ClpP protease activates nuclear genes involved in autophagy and plastid protein quality control. *Plant Cell*, **26**, 2201–2222.

Schmollinger, S., Mühlhaus, T., Boyle, N.R. *et al.* (2014) Nitrogen-sparing mechanisms in *Chlamydomonas* affect the transcriptome, the proteome, and photosynthetic metabolism. *Plant Cell*, **18**, 1410–1435.

Schneider, C. (2005) Chemistry and biology of vitamin E. *Mol. Nutr. Food Res.* **49**, 7–30.

Sewelam, N., Jaspert, N., Van Der Kelen, K., Tognetti, V.B., Schmitz, J., Frerigmann, H., Stahl, E., Zeier, J., Van Breusegem, F. and Maurino, V.G. (2014) Spatial H_2O_2 signaling specificity: H_2O_2 from chloroplasts and peroxisomes modulates the plant transcriptome differentially. *Mol. Plant*, **7**, 1191–1210.

Shao, N., Beck, C.F., Lemaire, S.D. and Krieger-Liszkay, A. (2008) Photosynthetic electron flow affects H_2O_2 signaling by inactivation of catalase in *Chlamydomonas reinhardtii*. *Planta*, **228**, 1055–1066.

Sobota, J.M. and Imlay, J.A. (2011) Iron enzyme ribulose-5-phosphate 3-epimerase in *Escherichia coli* is rapidly damaged by hydrogen peroxide but can be protected by manganese. *Proc. Natl Acad. Sci. USA*, **108**, 5402–5407.

Somanchi, A., Barnes, D. and Mayfield, S.P. (2005) A nuclear gene of *Chlamydomonas reinhardtii*, *Tba1*, encodes a putative oxidoreductase required for translation of the chloroplast *psbA* mRNA. *Plant J.* **42**, 341–352.

Stone, J.R. and Yang, S. (2006) Hydrogen peroxide: a signaling messenger. *Antioxid. Redox Signal.* **8**, 243–270.

Takeda, T., Yokota, A. and Shigeoka, S. (1995) Resistance of photosynthesis to hydrogen peroxide in algae. *Plant Cell Physiol.* **36**, 1089–1095.

Tietze, F. (1969) Enzymic method for quantitative determination of nanogram amounts of total and oxidized glutathione: applications to mammalian blood and other tissues. *Anal. Biochem.* **27**, 502–522.

Trapnell, C., Williams, B.A., Pertea, G., Mortazavi, A., Kwan, G., van Baren, M.J., Salzberg, S.L., Wold, B.J. and Pachter, L. (2010) Transcript assembly and quantification by RNA-Seq reveals unannotated transcripts and isoform switching during cell differentiation. *Nat. Biotechnol.* **28**, 511–515.

Urzica, E.I., Adler, L.N., Page, M.D., Linster, C.L., Arbing, M.A., Casero, D., Pellegrini, M., Merchant, S.S. and Clarke, S.G. (2012a) Impact of oxidative stress on ascorbate biosynthesis in *Chlamydomonas* via regulation of the *VTC2* gene encoding a GDP-L-galactose phosphorylase. *J. Biol. Chem.* **287**, 14234–14245.

Urzica, E.I., Casero, D., Yamasaki, H. *et al.* (2012b) Systems and trans-system level analysis identifies conserved iron deficiency responses in the plant lineage. *Plant Cell*, **24**, 3921–3948.

Vandenabeele, S., Van Der Kelen, K., Dat, J. *et al.* (2003) A comprehensive analysis of hydrogen peroxide-induced gene expression in tobacco. *Proc. Natl Acad. Sci. USA*, **100**, 16113–16118.

Vandenbroucke, K., Robbens, S., Vandepoele, K., Inzé, D., Van de Peer, Y. and Van Breusegem, F. (2008) Hydrogen peroxide-induced gene expression across kingdoms: a comparative analysis. *Mol. Biol. Evol.* **25**, 507–516.

Wakao, S., Chin, B.L., Ledford, H.K., Dent, R.M., Casero, D., Pellegrini, M., Merchant, S.S. and Niyogi, K.K. (2014) Phosphoprotein SAK1 is a regulator of acclimation to singlet oxygen in *Chlamydomonas reinhardtii*. *Elife*, **3**, e02286.

Walling, C. (1975) Fenton's reagent revisited. *Acc. Chem. Res.* **8**, 125–131.

Wu, A.L. and Moye-Rowley, W.S. (1994) *GSH1*, which encodes gamma-glutamylcysteine synthetase, is a target gene for yAP-1 transcriptional regulation. *Mol. Cell. Biol.* **14**, 5832–5839.

Wu, G., Hufnagel, D.E., Denton, A.K. and Shiu, S.H. (2015) Retained duplicate genes in green alga *Chlamydomonas reinhardtii* tend to be stress responsive and experience frequent response gains. *BMC Genom.* **16**, 149.

Zeller, T., Moskvin, O.V., Li, K., Klug, G. and Gomelsky, M. (2005) Transcriptome and physiological responses to hydrogen peroxide of the facultatively phototrophic bacterium *Rhodobacter sphaeroides*. *J. Bacteriol.* **187**, 7232–7242.

Zhu, Y., Graham, J.E., Ludwig, M., Xiong, W., Alvey, R.M., Shen, G. and Bryant, D.A. (2010) Roles of xanthophyll carotenoids in protection against photoinhibition and oxidative stress in the cyanobacterium *Synechococcus* sp. strain PCC 7002. *Arch. Biochem. Biophys.* **504**, 86–99.

Zones, J., Blaby, I., Merchant, S. and Umen, J. (2015) High-resolution diurnal transcriptome from *Chlamydomonas* reveals continuous cell and metabolic differentiation. *Plant Cell*, in press.